Site percolation and a spin-diffusion model as applied to Gd^{3+} EPR linewidth behaviour in $Pr_xLa_{1-x}F_3$ single crystals

1992 J. Phys.: Condens. Matter 4 6459

(http://iopscience.iop.org/0953-8984/4/30/012)

J. Phys.: Condens. Matter 4 (1992) 6459–6466. Printed in the UK

Site percolation and a spin-diffusion model as applied to Gd^{3+} EPR linewidth behaviour in $Pr_xLa_{1-x}F_3$ single crystals

Sushil K Misra and Ufuk Orhun

Physics Department, Concordia University, 1455 de Maisonneuve Boulevard West, Montreal, Quebec H3G 1M8, Canada

Received 24 March 1992

Abstract. The experimentally observed impurity-ion Gd^{3+} EPR linewidth behaviour in $Pr_xLa_{1-x}F_3$ host crystals as a function of x, the fraction of the host paramagnetic ions Pr^{3+}, has been shown to be satisfactorily explained by the formation of paramagnetic percolation clusters and the resulting spin diffusion.

1. Introduction

Spin lattice relaxation is a very complex process, governed by a number of mechanisms whose strengths depend very sensitively upon temperature, as well as upon the properties of the ions on the host lattice. When an impurity paramagnetic ion is introduced into a lattice, its electron paramagnetic resonance (EPR) linewidth may be dramatically influenced by the particular host lattice, especially when it contains paramagnetic ions. A number of mechanisms have been proposed, and their effect theoretically investigated, for the impurity-ion EPR linewidth; for a review see Abragam and Bleaney (1970). However, a satisfactory explanation of the behaviour of the observed impurity-ion EPR linewidth has not yet been fully accomplished in all cases. The percolation phenomenon has recently been applied successfully by Misra and Orhun (1990b) to explain the observed impurity-ion EPR linewidth behaviour in single crystals of Gd^{3+}-doped $LiYb_xY_{1-x}F_4$, which contain paramagnetic host ions (Yb^{3+}), as a function of x, the fraction of the host paramagnetic ions. Briefly, in this model, one calculates the value of x_c, the particular concentration of the host paramagnetic ions such that for $x > x_c$, the cluster formed by the connected paramagnetic host-ion sites extends all the way from one end of the crystal to the other, i.e. a paramagnetic percolation cluster exists. It is then expected that for $x > x_c$, the relaxation of the host paramagnetic ions due to the process of spin diffusion becomes fully effective. Thus, for those $LiYb_xY_{1-x}F_4$ crystals for which $x \geqslant x_c$, the EPR linewidths are expected to be highly temperature dependent, due to enhanced spin–lattice relaxation of the host paramagnetic ions. Specifically, the Gd^{3+} EPR linewidths in $LiYb_xY_{1-x}F_4$ as observed by Misiak *et al* (1988) were found to disappear at low temperatures for $x \geqslant 0.3$, while for $x < 0.3$ they could be clearly observed down to liquid helium temperature. Misra and Orhun (1990b) calculated x_c in $LiYb_xY_{1-x}F_4$ to be 0.27. Comparing this value with the observed Gd^{3+} linewidth behaviour as a function of x, it was established that the spin–lattice relaxation could take place via

0953-8984/92/306459+08$04.50

connected paramagnetic sites by the mechanism of spin diffusion, being effective only above the percolation threshold, i.e. for $x > 0.27$.

A variable-temperature EPR linewidth study of Gd^{3+}-doped $Pr_xLa_{1-x}F_3$ single crystals has recently been reported by Misra *et al* (1990a) in the temperature range 4.2–295 K. The behaviour of the reported Gd^{3+} EPR linewidths in $Pr_xLa_{1-x}F_3$ as a function of x, as exhibited in figure 1, is quite unusual. The experimental linewidth data can be divided according to x, the fraction of the host paramagnetic ions, Pr^{3+}, into three categories.

(i) $0 \leqslant x \leqslant 0.2$. In this range, Gd^{3+} EPR lines are well resolved and temperature independent; they show increased broadening with increasing value of x.

(ii) $0.2 < x < 0.8$. The EPR lines are too broad to be observed for these concentrations.

(iii) $0.8 \leqslant x \leqslant 1$. For these values of x, the EPR lines are observable at room temperature, becoming narrower with increasing value of x. They are temperature dependent, first narrowing with decreasing temperature and then broadening below certain temperatures, and finally becoming too broad at liquid helium temperatures to be observed.

The sudden disappearance of Gd^{3+} EPR lines in $Pr_xLa_{1-x}F_3$ at $x = 0.3$ as x increases from 0 suggests that the mechanism of EPR line broadening becomes effective somewhere between $x = 0.2$ and $x = 0.3$. As x is increased further, the sudden reappearance of EPR lines at $x = 0.8$ and further narrowing of lines with increasing values of x suggests that a mechanism of narrowing of lines apparently becomes effective somewhere between $x = 0.7$ and $x = 0.8$. The particularly drastic broadening of the linewidths for values of x between 0.2 and 0.3 implies the existence of a site-percolation phenomenon; on the other hand, the sudden narrowing of lines for values of x between 0.7 and 0.8 as x increases and further narrowing of lines with increasing values of x indicate that there occurs motional narrowing of lines due to the process of spin diffusion. Both of these effects—namely, paramagnetic percolation and motional narrowing due to spin diffusion—are caused by the host ions, Pr^{3+}, which exhibit Van Vleck paramagnetism as shown in section 3. Thus, as x is increased to above a critical value, x_c, the formation of a paramagnetic site-percolation cluster is achieved, and then for $x \gg x_c$ motional narrowing of lines due to the spin-diffusion mechanism becomes operative. These two mechanisms then provide a satisfactory explanation of the Gd^{3+} linewidth behaviour in $Pr_xLa_{1-x}F_3$ as a function of x.

It is the purpose of the present paper to apply the phenomenon of paramagnetic site percolation, in conjunction with the resulting spin diffusion, to explain the Gd^{3+} EPR linewidth behaviour as a function of the concentration x of the paramagnetic host ions Pr^{3+} in $Pr_xLa_{1-x}F_3$ single crystals. The details of the crystal structure of $Pr_xLa_{1-x}F_3$ single crystals required for the calculation of the percolation threshold x_c are given in section 2, followed by a discussion of paramagnetism of the Pr^{3+} ion in the lattice of $Pr_xLa_{1-x}F_3$ in section 3. Sections 4, 5 and 6, respectively, deal with the calculation of x_c, an explanation of the linewidth behaviour as governed both by paramagnetic percolation and motional narrowing due to spin diffusion, and the temperature dependence of the linewidth. A discussion and concluding remarks are included in section 7.

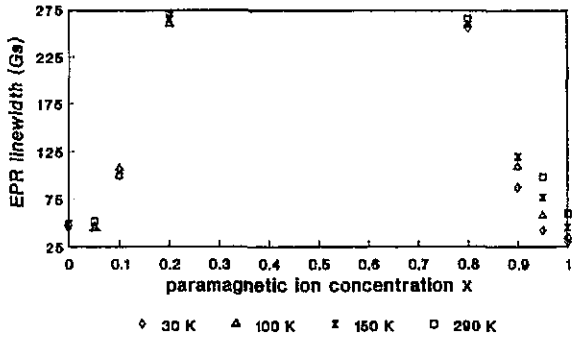

Figure 1. Averages of the experimentally observed Gd^{3+} EPR linewidths for the various transitions in $Pr_xLa_{1-x}F_3$ crystals at various temperatures as a function of x, the fraction of Pr^{3+} ions (Misra *et al* 1990).

2. Crystal structure

For the present calculations one needs to know the positions of the rare-earth ions in $Pr_xLa_{1-x}F_3$ single crystals. When a Gd^{3+} ion is introduced into the lattice of $Pr_xLa_{1-x}F_3$, it replaces one of the rare-earth ions. In the samples used for EPR data, there was present one Gd^{3+} ion for every 1000 rare-earth ions. $Pr_xLa_{1-x}F_3$ single crystals can be considered to be hexagonal with six molecules per unit cell; their unit-cell parameters can be calculated by interpolating linearly from those for LaF_3 and PrF_3 using Vegard's law (Vegard 1928). The unit-cell parameters for PrF_3 are: $a = 0.7061$ nm, $c = 0.7218$ nm, while they are: $a = 0.719$ nm, $c = 0.737$ nm for LaF_3 (Donnay and Donnay 1962). The six rare-earth ion sites are located at $(\frac{1}{3},\frac{1}{3},0)$, $(0,\frac{2}{3},0)$, $(\frac{2}{3},0,0)$, $(\frac{2}{3},\frac{2}{3},\frac{1}{2})$, $(0,\frac{1}{3},\frac{1}{2})$, and $(\frac{1}{3},0,\frac{1}{2})$ in the unit cell, as displayed in figure 2. It is noted that different rare-earth sites in the unit cell have different local surroundings. These sites are referred to as $1,2,\ldots,6$, respectively, in section 3.

3. Paramagnetism of the Pr^{3+} ion in the lattice of $Pr_xLa_{1-x}F_3$

The structure of $Pr_xLa_{1-x}F_3$ can be assumed to be the same as that of LaF_3. According to Matthies and Welsch (1975), the $^3H_4$ ground level of the non-Kramers ion Pr^{3+} splits, in the lattice of LaF_3, into nine singlets of energies: 0, 57, 76, 136, 195, 204, 296, 322, and 508 cm^{-1}. Thus, to zero order, the Pr^{3+} ion is non-magnetic in this lattice. However, it is paramagnetic for the following reason. It posseses Van Vleck paramagnetism, as clearly pointed out by Mehran and Stevens (1982) in the context of the $PrVO_4$ lattice. The present case can be compared with that of the $PrVO_4$ lattice where the $^3H_4$ ground level of Pr^{3+} splits into five singlets of energies: 0, 35, 127, 276 and 390 cm^{-1}, and two doublets of energies: 84 and 600 cm^{-1}. Since the splitting of the lowest levels of Pr^{3+} in LaF_3 is not large, the occupations of these levels would be quite significant even at temperatures above liquid helium temperature. Thus, they will contribute to the paramagnetism of the Pr^{3+} ion in this lattice, as seen by using the wavefunctions listed by Matthies and Welsch (1975). Such a temperature dependence is discussed by Mehran and Stevens (1982), as well as by Sugawara and Huang (1975).

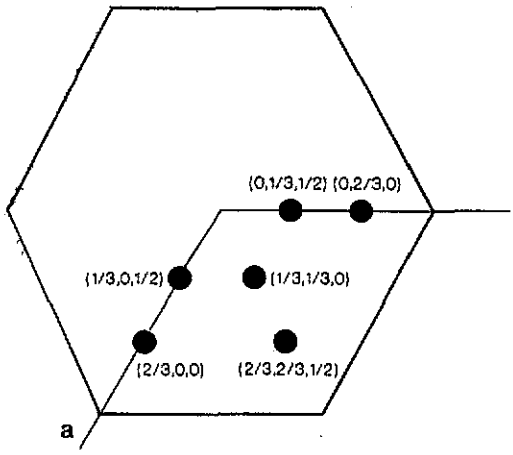

Figure 2. A $Pr_xLa_{1-x}F_3$ hexagonal unit cell showing sites occupied by the rare-earth ions, as projected onto the plane perpendicular to the c axis. The solid circles represent the rare-earth ions in the $z = 0$ plane, while the hatched circles represent those in the $z = 0.5c$ plane. (Here c is the unit-cell dimension.) The impurity Gd^{3+} ions replace a rare-earth ion when introduced into the lattice of $Pr_xLa_{1-x}F_3$.

That the Pr^{3+} ions exhibit paramagnetism is supported by the EPR linewidth data in the $Pr_xLa_{1-x}F_3$ lattice as discussed in section 1, and exhibited in figure 1. Specifically, in the purely diamagnetic lattice of LaF_3 ($x = 0$; the La^{3+} ion is diamagnetic) the linewidth is small and independent of temperature, whereas it increases for increasing value of x, representing the fraction of Pr^{3+} ions. Such behaviour is obviously due to the paramagnetism of the Pr^{3+} ion.

4. Calculation of percolation threshold

In this calculation an attempt was made to find if a path connecting paramagnetic Pr^{3+} ions exists all the way from one end of the lattice to the other. The following simulations for various values of x were performed on an IBM-AT computer. A $Pr_xLa_{1-x}F_3$ lattice was generated by using a $40 \times 40 \times 40$ array. A random-number generator was used to fill the array elements by Pr^{3+} and La^{3+} ions according to the particular value of x, representing the fraction of Pr^{3+} ions. The occupied paramagnetic sites were designated by the numbers 1–6, depending on to which one of the particular rare-earth site in the unit cell the occupied site corresponded, while the occupied diamagnetic sites were designated bu 0. First, all the sites occupied by the paramagnetic ions in the $z = 0$ plane (the plane at one extremity of the array considered), parallel to the (001) plane in the $Pr_xLa_{1-x}F_3$ lattice, were assumed to be connected to the paramagnetic cluster by designating them as 7–12, by adding 6 to their original values. Next, the sites in the $z = 1$ plane, lying within a distance r_L of a paramagnetic ion in the $z = 0$ plane, were checked to see if they were occupied by paramagnetic ions. (Here r_L determines connectivity as defined in the next paragraph.) The sites so occupied by paramagnetic ions were made a part of the paramagnetic cluster, and appropriately designated as 7–12. In this manner, all the sites in the various successive planes $z = 1$–39 were checked, and when qualified,

made a part of the cluster. The successive $z = 1, 2, 3, \ldots$ planes were defined to be the planes which are located at heights of $0.5c$, c, $1.5c$, ..., parallel to the $z = 0$ plane, because these are the planes in which the rare-earth ions are located. If, in the first sweep of $z = 1$ to 39 planes, it was found that a site in the $z = 39$ plane was connected to the cluster, the simulation was terminated, and it was concluded that a cluster extended all the way from one end of the sample to the other, i.e. the cluster was percolating. If this was not the case, a successive downward plane-wise sweep from the $z = 39$ to the $z = 0$ plane was performed in order to include more sites of the cluster which were missed in the first upward sweep; thus, the cluster formed in the first sweep could grow. After this, the sweep of successive z planes was repeated in the upward direction, then in the downward direction, and so on. These sweeps were continued until either (*a*) a site in the $z = 39$ plane became connected to the cluster, in which case it was concluded that the cluster was percolating, or (*b*) the cluster did not grow at all after two successive sweeps, i.e. an upward sweep followed by a downward sweep, in which case it was concluded that the cluster was not percolating, i.e. it did not extend all the way form one end of the sample to the other.

The simulations were performed for various values of x, and the values of x for which percolating clusters occurred were determined. The value of the threshold, i.e. x_c, above which percolation clusters occurred, was found to depend on the limiting distance r_L, or the connectivity, around a paramagnetic ion, within which the paramagnetic ions in the percolating cluster were included. In the present case, two different values of the limiting distance, r_L, were employed: (i) $r_L = 0.6$ nm and (ii) $r_L = 0.8$ nm. The percolation threshold x_c was found to be 0.48 ± 0.01 for case (i), while for case (ii) the value of x_c was found to be 0.21 ± 0.01. The decrease in the value of x_c for case (ii), as compared to that for case (i), is due to the increase in the number of connectable neighbours for case (ii). Finally, the value of $x_c = 0.21 \pm 0.01$ as found for case (ii) ($r_L = 0.8$ nm) appears to explain well the experimental data on Gd^{3+} EPR linewidths in $Pr_xLa_{1-x}F_3$ crystals as a function of x.

5. Spin diffusion

The observed behaviour of the Gd^{3+} EPR linewidth in $Pr_xLa_{1-x}F_3$ single crystals as a function of x, as described in section 1 and displayed in figure 1, can be qualitatively understood by invoking the theory of EPR linewidth in the presence of motion of spins as discussed by Abragam (1970), together with the treatment of dipolar broadening of a magnetic resonance line in a magnetically dilute crystal as provided by Kittel and Abrahams (1953).

Basically, as seen from figure 1 which shows experimental EPR linewidth data, at any temperature the observed Gd^{3+} EPR linewidth in $Pr_xLa_{1-x}F_3$ crystals increases as x increases from 0 to 0.2; thereafter it becomes too large for EPR lines to be observed for $0.2 < x < 0.8$. Finally, the linewidth decreases with increasing x for $x > 0.8$. The drastic increase of Gd^{3+} EPR linewidth at $x \sim 0.2$ as x incrases can be said to be due to paramagnetic percolation. On the other hand, the narrowing of EPR lines which begins at $x \sim 0.8$ as x increases can be said to be due to 'motional narrowing' in terms of spin diffusion as follows.

When the paramagnetic host-ion cluster is percolating ($x > x_c$), there occurs spin diffusion. Equivalently, there propagate throughout the lattice mutual spin flips

of neighbouring paramagnetic spins, wherein an upward-pointing spin flips downward and this is accompanied by the upward flip of a neighbouring downward-pointing spin. (It is assumed that the external Zeeman field is directed upward.) In this case, motional narrowing of EPR lines may take place. This happens when the average value of the local field experienced by a given spin, taken over a long time compared with the duration of fluctuation of the local field due to a neighbouring spin, is much smaller than the instantaneous value of the local field. The rate of fluctuations of the local field can be described by a correlation time, τ_c. The criterion for motional narrowing due to spin diffusion is then

$$\left(\overline{\Delta\omega_0^2}\right)^{1/2} \ll 1/\tau_c. \tag{1}$$

In equation (1), $\overline{\Delta\omega_0^2}$ is the Van Vleck second moment. On the other hand, when

$$\left(\overline{\Delta\omega_0^2}\right)^{1/2} \gg 1/\tau_c \tag{2}$$

there is a complete absence of motional narrowing; in other words, spin diffusion is not at all effective.

In order to get an estimate of τ_c needed in equations (1) and (2), one can express τ_c as

$$\tau_c = T_1 f(x) \tag{3}$$

where T_1 is the spin-lattice relaxation time of the host paramagnetic ions, which varies as x^{-1} (Kittel and Abrahams 1953), while $f(x)$ is a rapidly decreasing function of x as x increases from 0, being extremely large at $x = 0$, and becoming quite small asymptotically as $x \to 1$. Thus, equation (2) will be satisfied for $x \sim 1$, while equation (1) will be satisfied when $x \sim 0$. This is consistent with the observed linewidth behaviour exhibited in figure 1, which indicates the existence of motional narrowing of lines due to spin diffusion for $x \sim 1$. Further, for $x \sim 0$, it is noted that according to Kittel and Abrahams (1953) and Waller (1932), in the absence of exchange and hyperfine interactions, the linewidth $(\overline{\Delta\omega^2})^{1/2}$ for random occupancy is proportional to $x^{1/2}$ when $x > 0.1$, while it is proportional to x for $x < 0.02$.

Finally, the above considerations lead to the following expressions describing asymptotic linewidth behaviours for Gd^{3+} in $Pr_xLa_{1-x}F_3$.

(i) Absence of motional narrowing (x near 0):

$$\left(\overline{\Delta\omega^2}\right)^{1/2} = \left(\overline{\Delta\omega_0^2}\right)^{1/2} \propto x \text{ or } x^{1/2} \qquad \left(\overline{\Delta\omega_0^2}\right)^{1/2} \tau_c \gg 1. \tag{4}$$

(ii) Presence of motional narrowing (x near 1):

$$\left(\overline{\Delta\omega^2}\right)^{1/2} = \left(\overline{\Delta\omega_0^2}\right) \tau_c \propto x^{-\alpha} (\alpha > 0) \qquad \left(\overline{\Delta\omega_0^2}\right)^{1/2} \tau_c \ll 1. \tag{5}$$

The asymptotic linewidth behaviours indicated by equations (4) and (5) for $x \to 0$ and for $x \to 1$ are qualitatively in agreement with the experimentally observed room-temperature linewidth as a function of x as displayed in figure 1. Of course, for

intermediate values of x ($0.2 < x < 0.8$), the linewidth becomes too large to be observed due to paramagnetic percolation.

The role played by the percolation threshold, x_c, is as follows. For $x > x_c$ spin relaxation at one site is allowed to affect Gd^{3+} spins via spin diffusion over a macroscopic region. τ_c, which determines whether equation (4) or equation (5) is applicable, is not expected to change dramatically as one goes through the percolation limit x_c as expected from equation (3). Further, as x approaches x_c, the observed linewidth behaviour is not found to exhibit a jump at $x = x_c$, contrary to what is expected on the basis of the percolation threshold. This may be explained as being due to increased irregularity in the crystal lattice as Pr^{3+} ions substitute for La^{3+} ions, thereby smoothing the jump warranted by paramagnetic percolation.

6. Temperature variation of EPR linewidth in $Pr_xLa_{1-x}F_3$

Reference to figure 1 reveals that as the temperature is lowered from room temperature, the linewidths do not change for samples with $x < 0.2$, while they vary appreciably with temperature for samples with $x > 0.8$. Of course, they are too large to be observed at any temperature for $0.8 > x > 0.2$. The reason for temperature independence of linewidths for samples with $x < 0.2$ is that in this case spin diffusion is not operative, since $x < x_c$; also, the host ions are predominantly diamagnetic (La^{3+} ions). On the other hand, for samples with $x > 0.8$, paramagnetic percolation is fully effective, because there is a sufficient predominance of host paramagnetic ions (Pr^{3+}); this may result in a profound temperature dependence of the EPR linewidth. In addition, there are operative other temperature-dependent line broadening mechanisms; for more details see Misra *et al* (1990a).

7. Discussion and concluding remarks

From the present considerations, it can be concluded that the spin–lattice relaxation mechanism due to spin diffusion that is responsible for EPR line broadening is closely linked to the percolation properties of the paramagnetic host ions in the lattice. The calculated paramagnetic percolation threshold, x_c, above which the process of spin diffusion is effective, for the case when the connectivity is confined to neighbours located within a distance $r_L < 0.8$ nm, in conjunction with a simple theory as described by Abragam (1970), predicts quite well the observed Gd^{3+} EPR linewidth behaviour in $Pr_xLa_{1-x}F_3$ host crystals as a function of x.

Although the present calculations have been applied to a $40 \times 40 \times 40$ array, it is expected that for larger arrays the results will not be significantly different. The value of r_L, the connectivity, may be somewhat modified when the dimension approaches infinity to lead to the value of $x_c = 0.21$, required to explain the EPR linewidth data on Gd^{3+}-doped $Pr_xLa_{1-x}F_3$ single crystals.

It is hoped that application of the proposed model, taking into account the influence of paramagnetic percolating clusters, to more experimental EPR linewidth data in host crystals consisting of paramagnetic ions would put this model on a firmer footing. The present paper attempts to demonstrate, in a qualitative manner, the profound effect of the percolation and spin-diffusion mechanisms on EPR linewidth behaviour. It is hoped that the present results will stimulate more detailed quantitative treatments of linewidth behaviour based on the effect of formation of paramagnetic percolating clusters.

Acknowledgments

The authors are grateful to the Natural Sciences and Engineering Research Council of Canada (grant No 0GP0004485) for partial financial support.

References

Abragam A 1970 *The Principles of Nuclear Magnetism* (Oxford: Clarendon) pp 425–7
Abragam A and Bleaney B 1970 *Electron Paramagnetic Resonance of Transition Ions* (Oxford: Clarendon) pp 541–83
Donnay J D H and Donnay G 1962 *Crystal Data Determinative Tables* 2nd edn (New York: American Crystallographic Association)
Kittel C and Abrahams E 1953 *Phys. Rev.* **90** 238
Matthies S and Welsh D 1975 *Phys. Status Solidi* b **68** 125
Mehran F and Stevens K W H 1982 *Phys. Rep.* **85** 123
Misiak L E, Misra S K, and Mikolajczak P 1988 *Phys. Rev.* B **38** 8673
Misra S K, Korczak W, Korczak S Z and Subotowicz M 1990a *Solid State Commun.* **76** 1055
Misra S K and Orhun U 1990b *Phys. Rev.* B **41** 2577
Sugawara K and Huang C Y 1975 *Phys. Rev.* **11** 4455
Vegard L 1928 *Z. Crystallogr.* **67** 239
Waller I 1932 *Z. Phys.* **79** 370